43rd AIAA/ASME/SAE/ASEE Joint Propulsion Conference & Exhibit
8 - 11 July 2007, Cincinnati, OH

AIAA 2007-5267

Wall Sheath and Electron Mobility Modeling in Hybrid-PIC Hall Thruster Simulations

Richard R. Hofer,* Ioannis G. Mikellides,† Ira Katz,‡ and Dan M. Goebel§
Jet Propulsion Laboratory, California Institute of Technology, Pasadena, CA 91109

Progress on the development of physics-based modeling tools aimed at predicting the service life of Hall thrusters is discussed. Modifications of the wall sheath and electron mobility models in the hybrid fluid/particle-in-cell computer code HPHall-2 are made and the effects of these changes on the plasma parameters and thruster performance are assessed. The wall sheath model of Hobbs and Wesson [Plasma Physics, 9, 85-87 (1967)] has been adopted, resulting in modifications to the predicted sheath potentials that are relevant to the modeling of high specific impulse Hall thrusters. Experiments with a widely used mixed-mobility model of the cross-field electron transport is presented that enables the simultaneous prediction of thrust and discharge current in agreement with experimental data. Taken together, these code modifications have improved the predictive capability of HPHALL-2 to serve as an input for studies of Hall thruster erosion.

I. Introduction

MANY NASA science missions, such as those considered under the cost-capped Discovery program for example, require wider throttling capabilities and longer thruster life compared to commercial applications [1-3]. The service life of electric propulsion has been customarily demonstrated through life ground tests that typically cost several million dollars. The Extended Life Test of the 2.3 kW NSTAR ion thruster was completed in 2004 after more than 30,000 h of operation at the Jet Propulsion Laboratory (JPL), and was the longest life test of an ion thruster ever conducted [4]. In 2005, Aerojet demonstrated 5,800 h of operation of a BPT-4000 as part of a qualification program for geosynchronous earth orbit (GEO) applications [5,6]. The potential benefits for Discovery-class missions prompted NASA to fund a

* Member of the Technical Staff, Electric Propulsion Group, Propulsion and Materials Engineering Section, 4800 Oak Grove Drive, Mail Stop 125-109; richard.r.hofer@jpl.nasa.gov. Senior Member AIAA.

† Member of the Technical Staff, Electric Propulsion Group, Propulsion and Materials Engineering Section. Senior Member AIAA.

‡ Group Supervisor, Electric Propulsion Group, Propulsion and Materials Engineering Section. Senior Member AIAA.

§ Senior Research Scientist, Propulsion and Materials Engineering Section. Senior Member AIAA.

low-power life test extension of this thruster that added 950 h of operation at 1-2 kW discharge power, thereby extending the qualified throttling range of this thruster from 1 to 4.5 kW [7]. As NASA missions become more demanding both the cost and time associated with life tests is expected to rise. While some flagship missions may be able to absorb such costs, launch window opportunities and mission timelines may simply rule out long-duration life testing regardless of the mission class.

Two major life-limiting mechanisms exist in Hall thrusters: erosion of the discharge chamber walls and erosion of the hollow cathode. To better understand these mechanisms the computational effort at JPL has made use of existing models [8,9] wherever applicable, and has developed new models or extensions to existing models as deemed necessary [10-14]. In this paper, we report on efforts to improve our discharge chamber models used for simulating performance and erosion. This is a continuation of previous works reported in Ref. [11,12] that utilized a modified version of HPHALL-2 [8,9]. HPHall is an axisymmetric solver that employs a hybrid fluid/particle-in-cell (hybrid-PIC) numerical approach to simulate the evolution of the plasma inside the discharge chamber and near plume regions of a Hall thruster. HPHALL, originally developed by Fife and Martínez-Sánchez [8], was recently upgraded by Parra and Ahedo [9], resulting in the latest release, HPHALL-2. Throughout this paper, we report results using HPHALL-2 with additional JPL modifications.

In this paper, we present changes made to the wall sheath and electron mobility models in HPHall-2. A minor revision is made to the wall sheath model that results in changes to the predicted sheath potentials that are important when modeling high specific impulse Hall thrusters. A mixed mobility model for the cross-field electron transport is also considered that allows for the simultaneous matching of the thrust and discharge current. The effects of the code modifications on the plasma properties and predicted performance are assessed relative to prior experimental and numerical results. Overall, the updates to the wall sheath and electron mobility models have improved the predictive capability of HPHALL-2 to model Hall thruster physics, thereby increasing our confidence in the code as an input to erosion calculations.

II. Model Inputs

All results in this paper are based on the SPT-100 geometry and magnetic field used previously in Ref. [12]. Figure 1 shows the geometry and grid and Table 1 presents some of the basic inputs used for the simulations. Figure 2 shows the normalized magnetic field intensity on discharge chamber centerline from Ref. [15]. A similar magnetic field profile and topography (not shown) are used in the present results. We have updated the secondary electron emission (SEE) yield from those used in Ref. [12] to values found in Ref. [16] for borosil ($BNSiO_2$). The SEE yield is given by

$$\delta_w\left(T_e\right) = \Gamma\left[2+b\right] a T_e^b , \tag{1}$$

where Γ is the gamma function, T_e is the electron temperature, and a and b are coefficients fit to the data in Ref. [17]. Numeric values for the fit coefficients are given in Table 1.

Table 1. HPHALL inputs for plasma simulations.

Parameter	Value
Discharge Voltage (V)	300
Mass flow rate (mg/s)	5
Anode temperature (K), [18,19]	750
Wall temperature (K), [18,19]	850
Channel outer diameter (mm)	100
Channel width (mm)	15
Channel length (mm)	25
Simulation time step (s)	5e-8
SEE Yield Coefficient "a" [17]	0.123
SEE Yield Coefficient "b" [17]	0.528

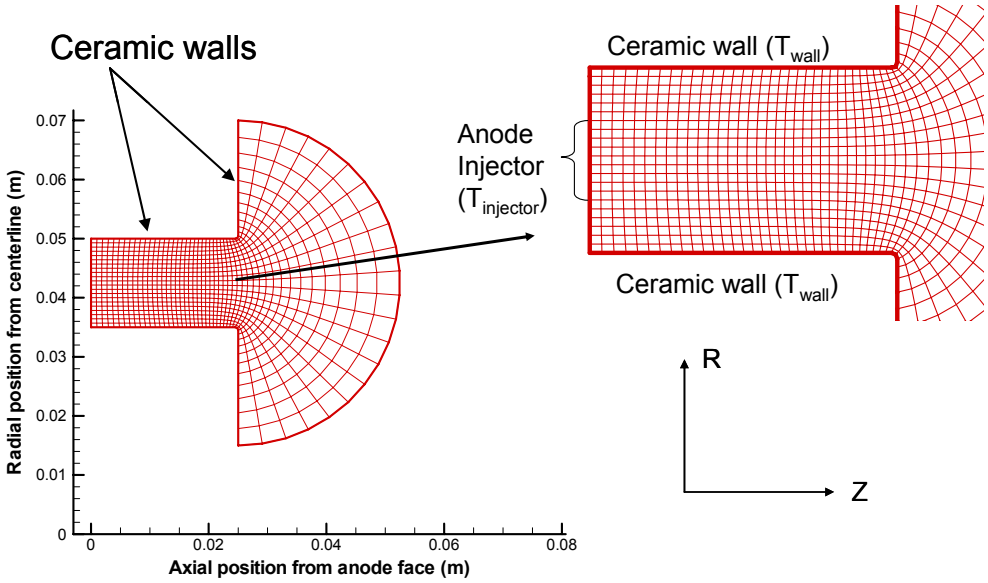

Figure 1. Geometry and grid used for plasma simulations with HPHALL.

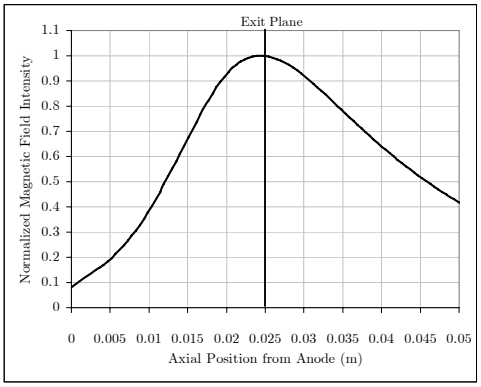

Figure 2. Normalized intensity of the magnetic field on discharge chamber centerline from Ref. [15].

III. Wall Sheath Modeling

The performance and erosion of a Hall thruster are strongly affected by the plasma sheath of the dielectric walls. As such, a physically representative model of the wall sheath is needed if accurate predictions of performance and erosion are to be obtained. Understanding of wall sheath physics in Hall thrusters has been considerably advanced in the last several years and continues to be the subject of research [20-29]. The complexity of the physics and the uncertainty in key physical parameters (e.g., the secondary electron emission yield [16,17,20,29-32]) has resulted in several models being proposed that can differ substantially in their assumptions and results. While presently there is a dearth of consensus on an appropriate model, the model proposed by Ahedo in Ref. [33] was a significant step forward when introduced to HPHALL-2 in Ref. [9].

Ahedo's sheath model is a generalization of the model proposed by Hobbs and Wesson (H&W) [34] for warm ions drifting supersonically between annular walls. To satisfy the Bohm sheath condition, Ahedo's model introduces separate electron populations for the bulk plasma and the sheath at temperatures T_e and T_p, respectively. This approach leads to a non-physical loss of energy across the sheath/pre-sheath boundary that is especially important near the charge saturation limit (CSL). To avoid this, we have reverted to the sheath model of H&W, which is recovered from Ahedo's sheath model by allowing T_p=T_e.

An important assumption of these models is that secondary electrons emitted from the wall are completely thermalized with the bulk plasma after leaving the sheath. Research presented in Ref. [23,26,28] have questioned whether this assumption is valid for Hall thruster plasmas. While these works have shown that this assumption has limitations the research is still evolving and has not yet considered in detail how magnetic field effects (e.g., magnetic mirroring or the field line topography) may influence the thermalization of electrons. The importance of the magnetic field in regulating the electron current in Hall thrusters is now well established [35,36]. Consequently, we have chosen to retain the assumption of 100% SEE thermalization pending further advances. Additionally, the inclusion of doubly-charged ions and supersonic ions entering the sheath remains the subject of further work [25].

We have solved the model of H&W numerically in order to obtain the sheath parameters. Figure 3 shows the sheath potential and ion velocity entering the sheath as a function of the SEE yield. In HPHALL-2, the sheath potential dependence on the SEE yield is implemented by fitting the numerical solution shown in Figure 3 via

$$\phi = \ln\left(A\left(1-\delta_w\right)\right) - \frac{B}{\left(1-\delta_w\right)^2} - \frac{C}{\left(1-\delta_w\right)^3} - \frac{D}{\left(1-\delta_w\right)^4}, \tag{2}$$

where the coefficients are given in
Table 2.

An approximate expression for the sheath potential is given by

$$\hat{\phi}_{WQ} \equiv -\frac{e\phi_{WQ}}{kT_p} = \ln\sqrt{\frac{m_i}{2\pi m_e}} + \ln\left(1-\delta_w\right) + \ln\left(\frac{n_{pQ}}{n_{iQ}}\right) + \ln\left(\frac{v_{Bohm}}{v_{riQ}}\right), \tag{3}$$

where W denotes the wall, Q is the pre-sheath/sheath boundary, and the rest of the symbols have their usual meaning. The sheath potential is most strongly affected by the first two terms on the right hand side of the above equation until the CSL is nearly reached when the last term provides an important modification. At the CSL for a xenon plasma, each of the terms have numeric values given by

$$\underbrace{-\frac{e\phi_{WQ}}{kT_p}}_{-1.018} = \underbrace{\ln\sqrt{\frac{m_i}{2\pi m_e}}}_{5.274} + \underbrace{\ln\left(1-\delta_w\right)}_{-4.092} + \underbrace{\ln\left(\frac{n_{pQ}}{n_{iQ}}\right)}_{-0.019} + \underbrace{\ln\left(\frac{v_{Bohm}}{v_{riQ}}\right)}_{-0.145}. \tag{4}$$

Additionally, at the CSL for a xenon plasma, we have

$$\begin{aligned} &\delta_w = \delta_w^* = 1 - 8.3\sqrt{\frac{m_i}{m_e}} = 0.983 \\ &\frac{e\phi_{WQ}}{kT_e} = 1.018 \\ &E = \frac{1}{2}m_i v_{riQ}^2 = 0.578\ kT_e \\ &\Rightarrow v_{riQ} = 1.156\sqrt{\frac{T_e}{m_i}} = 1.156\ v_{Bohm} \end{aligned} \quad . \tag{5}$$

Note that at the CSL that the minimum ion velocity entering the sheath is 15.6% higher than the Bohm velocity.

Table 2. Coefficients for Eqn. (2).

A =	195.744
B =	1.289710E-04
C =	-3.454640E-06
D =	3.685070E-08

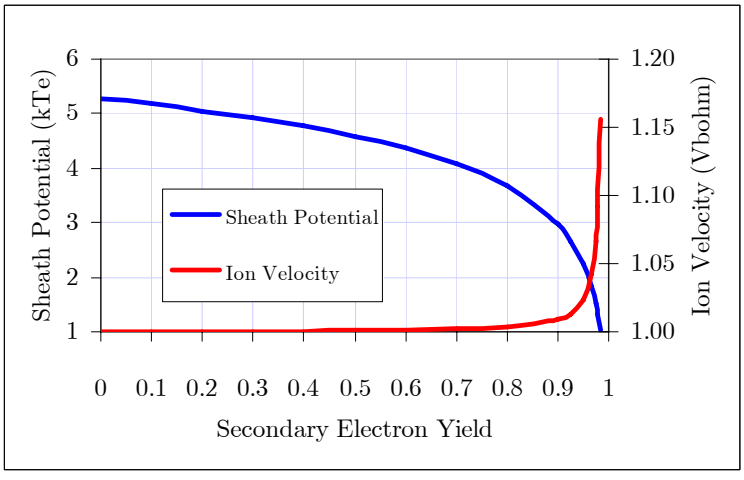

Figure 3. Sheath potential and ion velocity entering the sheath as a function of SEE yield.

Figure 4 compares the H&W solution we have implemented to the Ahedo sheath model. Note that the solutions are identical until the electron temperature approaches the first crossover energy of the wall material, that is, when the SEE yield approaches 100%. The H&W solution implemented here results in reduced sheath potentials, which in turn modifies the particle and energy fluxes to the walls (not shown). The importance of these changes will manifest at higher discharge voltages when the wall sheaths are in the CSL. Accurate modeling of the CSL is needed when modeling high specific impulse Hall thrusters such as NASA's HIVHAC or Aerojet's BPT-4000.

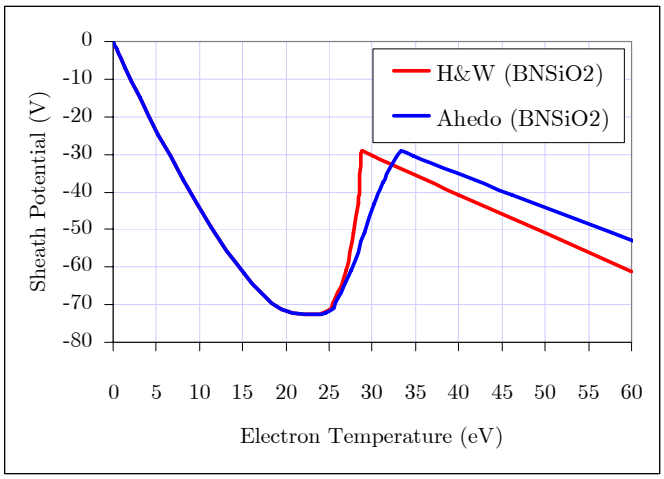

Figure 4. Sheath potential versus electron temperature from the sheath models of Ahedo [33] and Hobbs and Wesson [34].

Figure 5 and Figure 6 show the sheath potential and ion velocity entering the sheath, respectively, using the H&W sheath model. Note that the sheath potential is around 70 V over the last 5 mm of the channel, which will provide an additional 10,000 m/s of velocity to the ions as they traverse the sheath. In contrast, the ions entering the sheath do not attain a velocity of greater than 10,000 m/s until the last millimeter of the channel. Thus, the sheath potential is providing a significant fraction of the total velocity of ions that impact the wall and is therefore a critical aspect of any erosion calculation.

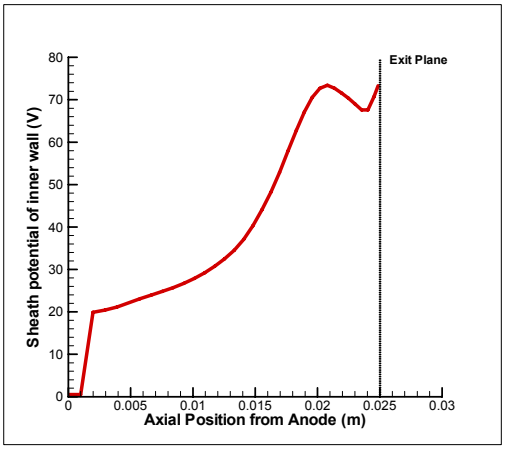

Figure 5. Axial variation of the sheath potential along the inner wall of the discharge chamber.

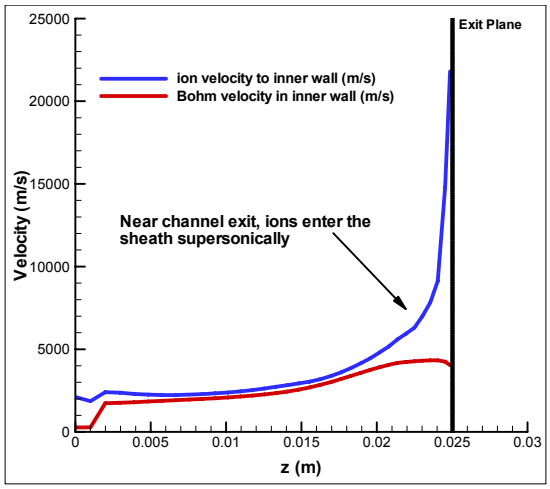

Figure 6. Average velocity of ions entering the sheath along the inner wall of the discharge chamber. The Bohm velocity is shown for reference. Near the channel exit, ions enter the sheath supersonically.

IV. Electron Mobility Modeling

In previous work [12], we reported on preliminary efforts to modify the electron mobility model used in HPHALL-2 with the aim of more accurately reproducing the spatial and temporal distributions of the plasma parameters. A review of mobility modeling research was also provided in Ref. [12] that will not be repeated here.

The axial, or cross-field, electron mobility is given by

$$\mu_{ez} = \frac{e}{\nu_e m_e}\left(\frac{1}{1+\Omega_e^2}\right), \tag{6}$$

which can be simplified to

$$\mu_{ez} \approx \frac{e}{\nu_e m_e \Omega_e^2} = \frac{\nu_e m_e}{eB_r^2} \quad , \tag{7}$$

since the electron Hall parameter is much greater than unity throughout the simulation domain [37-39]. Wall collisions and turbulent plasma fluctuations are known to enhance the cross-field mobility in Hall thrusters. While a determination of the dominant role of each of these mechanisms is beyond the scope of this paper, it is worth emphasizing that experimental, numerical simulation, and theoretical research [8,17,20,21,27,37-50], indicates that both mechanisms play a role in different regions of the simulation domain and at different thruster operating conditions. Including these effects in the mobility can be accomplished by using an effective electron collision frequency given by

$$\nu_e = \nu_{eff} \equiv \nu_{en} + \nu_{ei} + \nu_w + \nu_b \ , \tag{8}$$

where ν_{en} is the electron-neutral collision frequency, ν_{ei} is the electron-ion collision frequency, ν_w is the collision frequency of the electrons with the lateral walls (i.e., near-wall conductivity), and ν_b is a collision frequency defined to capture the bulk effects of turbulent plasma fluctuations.

The wall collision frequency is modeled in HPHALL-2 as

$$\nu_w = \frac{1}{\Delta \mathrm{V}} \left[\frac{\Delta A}{n_e} \Gamma_{rsW} \right] S_3 \bigcup S_4 = \frac{1}{\Delta \mathrm{V}} \left[\frac{\Delta A}{n_e} \frac{\delta_w}{1-\delta_w} \Gamma_{riQ} \right] S_3 \bigcup S_4 \,, \tag{9}$$

where ΔA and ΔV are area and volume elements between a pair of magnetic field lines sharing area elements S_3 and S_4 and the rest of the symbols have their usual meaning [9]. It is also worth noting that, for a channel of width h, the above expression simplifies to

$$\nu_w \approx \frac{2\delta_w}{h\left(1-\delta_w\right)} \sqrt{\frac{kT_e}{m_i}} \,, \tag{10}$$

when the radial magnetic field is purely radial, the wall sheaths are symmetric, and the ion velocity entering the sheath is sonic.

Anomalous Bohm-like diffusion is included in the expression for the effective collision frequency (Eqn. (2)) by supposing

$$\nu_b = \frac{1}{16} \alpha \omega_{ce} \,, \tag{11}$$

where α is a parameter that can be adjusted to match experiment so that the necessary amount of cross-field diffusion results. In the case of classic Bohm diffusion, α would be equal to 1.

In practice, assuming only near-wall conductivity or turbulent diffusion throughout the simulation domain is poorly justified by the available data. Instead, more physically realistic results may be achieved through the use of so-called mixed mobility models that discretize the axial variation of the parameter α into two or more zones [47,48]. Experiments suggest that α varies between the plasma bounded by the discharge chamber walls and the plasma expanding downstream of the channel exhaust [37-39]. In Ref. [12], we reported on a mixed-mobility approach, similar to Hagelaar, et al. and Koo, et al. [47,48], and have since performed additional numerical experiments. Specifically, turbulent fluctuations are modeled in two distinct regions separated by the exit plane of the discharge chamber. That is, we define α according to

$$\nu_t = \begin{cases} \frac{1}{16} \alpha_{dc} \omega_{ce} & z \le L \\ \frac{1}{16} \alpha_p \omega_{ce} & z > L \end{cases} \,, \tag{12}$$

where α_{dc} and α_p are parameters for the discharge chamber and plume, respectively, z is axial position, and L is the length of the discharge chamber. In practice, due to the disparity in the different parameters, the value of α is allowed to linearly vary over the first two or three field lines (about 1 to 2 mm), in order to smooth the transition between the two values of α.

In Ref. [12], it was found that using the mixed-mobility model with $\alpha_{dc}=0.1$ and $\alpha_p=0.2$ resulted in spatial distributions of the electron temperature and electric field that were more consistent with experiment, but with lower magnitudes. Additional numerical experiments have since shown that setting $\alpha_{dc}=0.035$ and $\alpha_p=1.0$, results in both good spatial distributions and magnitudes. Further, these choices

allow for simultaneous matching of the predicted discharge current and thrust (see section V below for more), which has sometimes been reported in the literature as difficult to do with mixed-mobility models [48].

Figure 7 and Figure 8 compares electron temperature and axial electric field predictions from the original version of HPHALL-2 with the standard mobility model (i.e., α=*0.1* everywhere) and from HPHALL-2 with the mixed mobility model using α_{dc}=*0.035* and α_{p}=*1.0*. The original version predicts peak electron temperature and electric field strengths downstream of the exit plane, which is not consistent with experimental data [21,27,37-39,51-53]. The mixed mobility model in the current version more correctly places the peak electron temperature and electric field inside the discharge chamber. The maximum electron temperatures are 30 and 26 eV for the original and current versions, respectively, which are both consistent with experiments that typically report peak electron temperatures that are around 10% of the discharge voltage [21,27,37-39,51-53].

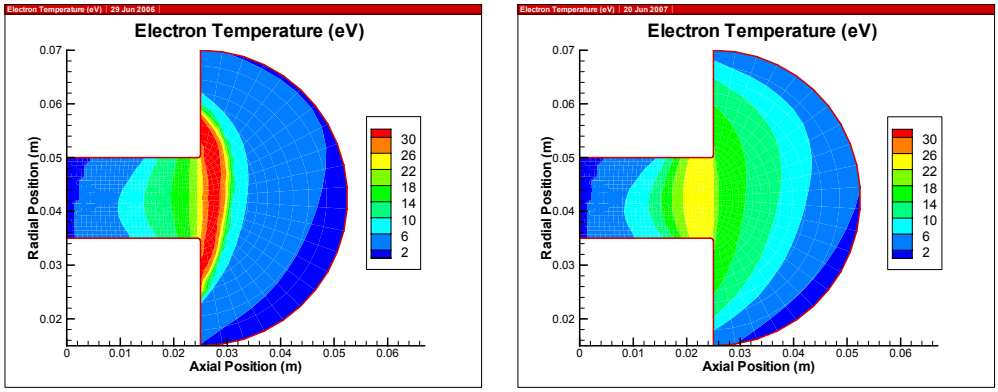

Original HPHALL-2 Current HPHALL-2

Figure 7. Electron temperature contours from HPHALL-2 with different mobility models. Maximum electron temperatures are 30 eV in the original version and 26 eV in the current version. (T_e ∈ [2, 30] eV)

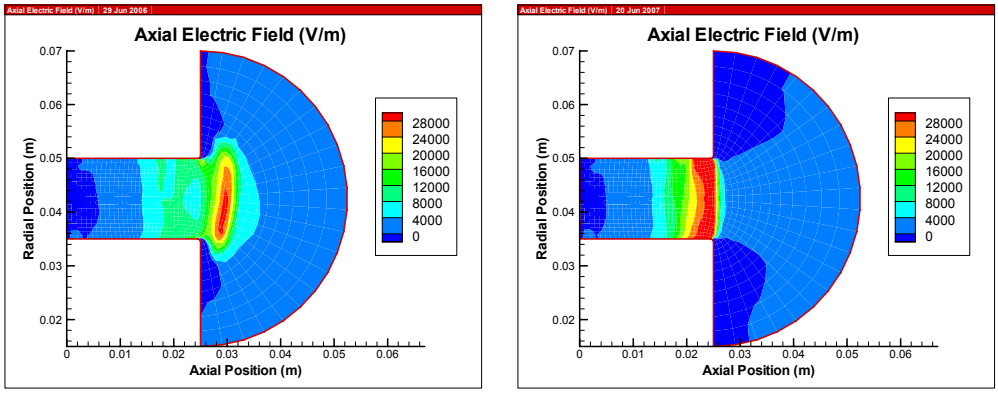

Original HPHALL-2 Current HPHALL-2

Figure 8. Axial electric field contours from HPHALL-2 with different mobility models. (E_z ∈ [0, 28000] V/m)

Note that setting $\alpha_p=1.0$, is equivalent to imposing "pure" Bohm diffusion in the plume. Doing so substantially lowers the plasma resistivity, and as shown in Figure 7 and Figure 8, this in turn quenches the electric field and keeps the electron temperature low in the plume region. Not until the electrons enter the discharge chamber do they encounter a significant electric field, consistent with experiment, where joule heating raises their temperature to a peak coinciding roughly with the peak in the axial variation of the radial magnetic field [21,27].

Figure 9 shows the collision frequency, averaged over magnetic field lines, as a function of axial position for HPHALL-2 using the mixed mobility model. The domain can roughly be divided into three regions. Deep in the channel near the anode the collision frequency is dominated by electron-neutral collisions due to the high neutral density in this region. Near the vicinity of the exit plane where the electric and magnetic fields are near their peaks, the turbulent collision frequency is greatest, while the electron-neutral and electron-wall collisions are of nearly equal value. Downstream of the exit plane, the collision frequency is entirely dominated by the turbulent collision frequency. Throughout the simulation domain, electron-ion collisions are negligible. Note that the effect of adding the turbulent collision frequency in the discharge chamber is to maintain a roughly constant value of the total collision frequency, whereas in the plume an enormous jump in the collision frequency is needed to obtain results consistent with experiment (i.e., low electric field and electron temperature).

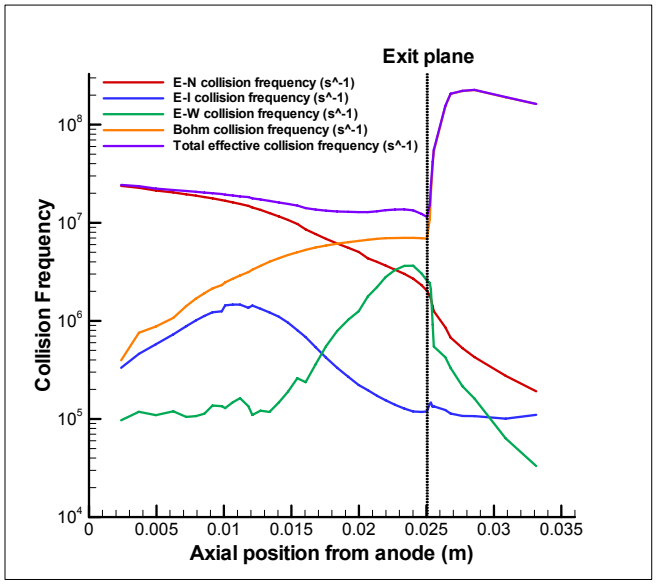

Figure 9. Collision frequency, averaged over magnetic field lines, as a function of axial position for HPHALL-2 using the mixed mobility model.

V. Plasma Response and Performance Predictions

Improvements in the wall sheath and electron mobility have improved the capability of HPHALL-2 to predict plasma properties and thruster performance consistent with experimental measurements. Figure 10 and Figure 11 show 1- and 2-dimensional profiles, respectively, of the neutral density, plasma density,

plasma potential, and electron temperature. Table 3 compares the predicted performance from the original and current versions of HPHALL-2 to experimental values from an SPT-100. These results increase our confidence in the code to predict accurately the inputs needed for erosion calculations.

The plasma properties predicted by the code are in good agreement with experimental measurements of the SPT-100 and other Hall thrusters [21,27,37-39,41,51-53] as well as plasma simulations of the SPT-100 [15,47,49,50]. The plasma response exhibits a high neutral density at the anode that decays monotonically due to the effects of ionization, a peak in the plasma density occurring approximately two-thirds of the channel length downstream of the anode, a peak in the electron temperature occurring near the maximum in the magnetic field profile, and a plasma potential profile that begins to decrease near the peak of the plasma density (i.e., an electric field profile that closely follows the magnetic field profile).

The thruster performance predicted by the code has also been improved from the original version. The original HPHALL-2, which used the standard mobility model, could not simultaneously match the discharge current and thrust. This situation leads to some uncertainty in the accuracy of any resulting erosion calculations due to the dependence of erosion processes on both the ion dynamics (via the thrust) and electron dynamics (via the discharge current). Any erosion simulation that does not provide adequate prediction of thrust and discharge current, regardless of the supposed agreement of the predicted sputtering with respect to experimental data, is of limited utility as a predictive tool. Despite these advances, detailed comparisons of the plasma response predicted by HPHALL-2 and experimental data are still needed (due to the wide range of SPT-100 models that are reported in the literature this is not possible). In the future, detailed comparisons of experimentally measured plasma properties, performance, and erosion will be conducted using a new high-power Hall thruster that has been designed for the purpose of conducting detailed physics investigations and benchmarking studies.

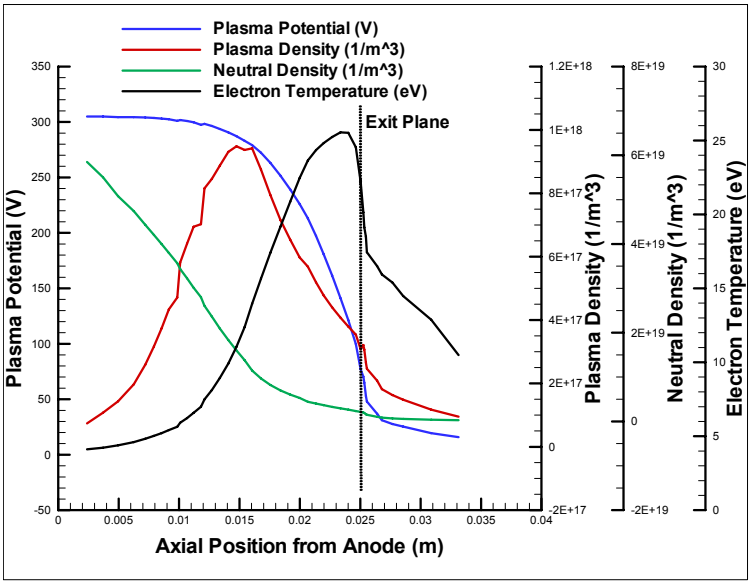

Figure 10. Axial dependence of the neutral density, plasma density, plasma potential, and electron temperature, averaged over magnetic field lines, from HPHALL-2 simulations.

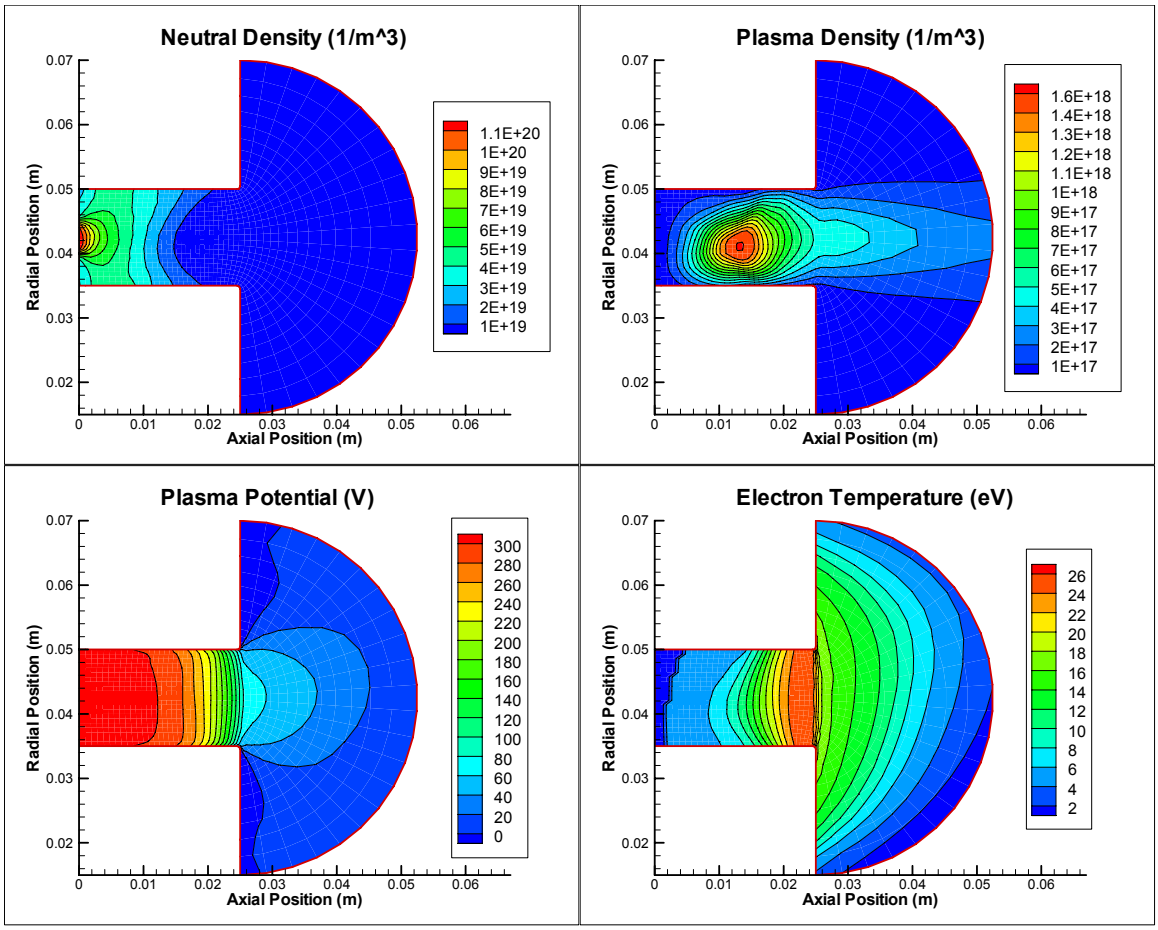

Figure 11. Neutral density, plasma density, plasma potential, and electron temperature from HPHALL-2 simulations.

Table 3. SPT-100 performance from experiment and the original and current versions of HPHALL-2. Modifications to the wall sheath and mobility model have improved the predictive capabilities of thruster performance, increasing confidence in the code to predict accurately the inputs needed for erosion calculations.

	Discharge current (A)	Thrust (mN)	Anode Efficiency
SPT-100 (measured)	4.5	85	55%
HPHALL-2 (original version)	4.4	70	39%
HPHALL-2 (current version)	4.5	85	55%

VI. Conclusion

Updates to the wall sheath and electron mobility models in HPHALL-2 have been made with the aim of increasing the accuracy of the plasma response and performance predictions in order to improve the inputs needed for erosion calculations. The use of the Hobbs and Wesson sheath model results in minor changes to the predicted sheath potentials that are relevant when modeling high specific impulse Hall thrusters. Numerical experiments with a mixed-mobility model of the cross-field electron transport have shown how the judicious choice of mobility parameters can lead to simultaneous matching of the thrust and discharge current. Taken together, these code modifications increase our confidence in the code to predict accurately the inputs needed for erosion calculations.

Despite being the most studied Hall thruster in the literature, the lack of a consistent set of internal plasma measurements of the SPT-100 limit our ability to rigorously validate the outputs from HPHALL-2. A new high-power Hall thruster has recently been tested that aims to ameliorate this situation through the availability of detailed design information, performance characterizations, internal and plume plasma data, and erosion studies. This new data will be critically important in the development of plasma and erosion Hall thruster models with the predictive capabilities needed in order to validate the service life of these devices for NASA science missions.

Acknowledgments

The research described in this paper was carried out at the Jet Propulsion Laboratory, California Institute of Technology, under a contract with the National Aeronautics and Space Administration. A portion of this work was supported by the NASA In-Space Propulsion program and was managed by Eric Pencil (NASA GRC), technology area manager for Solar Electric Propulsion.

References

[1] Hofer, R. R., Randolph, T. M., Oh, D. Y., Snyder, J. S., and de Grys, K. H., "Evaluation of a 4.5 kW Commercial Hall Thruster System for NASA Science Missions," AIAA Paper 2006-4469, July 2006.

[2] Oh, D. Y. and Goebel, D. M., "Performance Evaluation of an Expanded Throttle Range XIPS Ion Thruster System for NASA Science Missions," AIAA Paper 2006-4466, July 2006.

[3] Oh, D. Y., "Evaluation of Solar Electric Propulsion Technologies for Discovery-Class Missions," Journal of Spacecraft and Rockets **44**, 2, 399-411 (2007).

[4] Sengupta, A., Brophy, J. R., Anderson, J. R., Garner, C., de Groh, K. et al., "An Overview of the Results from the 30,000 Hr Life Test of Deep Space 1 Flight Spare Ion Engine," AIAA Paper 2004-3608, July 2004.

[5] de Grys, K. H., Welander, B., Dimicco, J., Wenzel, S., Kay, B. et al., "4.5 kW Hall Thruster System Qualification Status," AIAA Paper 2005-3682, July 2005.

[6] Welander, B. A. and de Grys, K. H., "Completion of the BPT-4000 Hall Thruster Qualification," Presented at the 53rd JANNAF Propulsion Meeting, Monterey, CA, Dec. 5-8, 2005.

[7] Welander, B., Carpenter, C., de Grys, K. H., Hofer, R. R., Randolph, T. M. et al., "Life and Operating Range Extension of the BPT-4000 Qualification Model Hall Thruster," AIAA Paper 2006-5263, July 2006.

[8] Fife, J. M., "Hybrid-PIC Modeling and Electrostatic Probe Survey of Hall Thrusters," Ph.D. Thesis, Aeronautics and Astronautics, Massachusetts Institute of Technology, 1998.

[9] Parra, F. I., Ahedo, E., Fife, J. M., and Martinez-Sanchez, M., "A Two-Dimensional Hybrid Model of the Hall Thruster Discharge," Journal of Applied Physics **100**, 023304 (2006).

[10] Mikellides, I. G., Katz, I., Goebel, D. M., and Polk, J. E., "Hollow Cathode Theory and Experiment. II. A Two-Dimensional Theoretical Model of the Emitter Region," Journal of Applied Physics **98**, 113303 (2005).

[11] Gamero-Castano, M. and Katz, I., "Estimation of Hall Thruster Erosion Using Hphall," Presented at the 29th International Electric Propulsion Conference, IEPC Paper 2005-303, Princeton, NJ, Oct. 31-Nov. 4, 2005.

[12] Hofer, R. R., Katz, I., Mikellides, I. G., and Gamero-Castano, M., "Heavy Particle Velocity and Electron Mobility Modeling in Hybrid-PIC Hall Thruster Simulations," AIAA Paper 2006-4658, July 2006.

[13] Mikellides, I. G., Katz, I., Goebel, D. M., and Jameson, K. K., "Evidence of Nonclassical Plasma Transport in Hollow Cathodes for Electric Propulsion," Journal of Applied Physics **101**, 063301 (2007).

[14] Mikellides, I. G., Katz, I., Goebel, D. M., Polk, J. E., and Jameson, K. K., "Plasma Processes inside Dispenser Hollow Cathodes," Physics of Plasmas **13**, 063504 (2006).

[15] Garrigues, L., Hagelaar, G. J. M., Bareilles, J., Boniface, C., and Bouef, J. P., "Model Study of the Influence of the Magnetic Field Configuration on the Performance and Lifetime of a Hall Thruster," Physics of Plasmas **10**, 12, 4886-4892 (2003).

[16] Viel-Inguimbert, V., "Secondary Electron Emission of Ceramics Used in the Channel of SPT," Presented at the 28th International Electric Propulsion Conference, IEPC Paper 2003-258, Toulouse, France, Mar. 17-23, 2003.

[17] Gascon, N., Dudeck, M., and Barral, S., "Wall Material Effects in Stationary Plasma Thrusters I: Parametric Studies of an SPT-100," Physics of Plasmas **10**, 10, 4123-4136 (2003).

[18] Arkhipov, B. A., Krochak, L. Z., Kudriavtsev, S. S., Murashko, V. M., and Randolph, T., "Investigation of the Stationary Plasma Thruster (SPT-100) Characteristics and Thermal Maps at the Raised Discharge Power," AIAA Paper 98-3791, July 1998.

[19] Arkhipov, B. A., Krochak, L. Z., and Maslenikov, N. A., "Thermal Design of the Electric Propulsion System Components: Numerical Analysis and Testing at Fakel," AIAA Paper 98-3489, July 1998.

[20] Barral, S., Makowski, K., Peradzynski, Z., Gascon, N., and Dudeck, M., "Wall Material Effects in Stationary Plasma Thrusters II: Near-Wall and in-Wall Conductivity," Physics of Plasmas **10**, 10, 4137-4152 (2003).

[21] Raitses, Y., Staack, D., Keidar, M., and Fisch, N. J., "Electron-Wall Interaction in Hall Thrusters," Physics of Plasmas **12**, 057104 (2005).

[22] Keidar, M., Boyd, I. D., and Beilis, I. I., "Plasma Flow and Plasma--Wall Transition in Hall Thruster Channel," Physics of Plasma **8**, 12, 5315-5322 (2001).

[23] Ahedo, E. and Parra, F. I., "Partial Trapping of Secondary-Electron Emission in a Hall Thruster Plasma," Physics of Plasmas **12**, 073503 (2006).

[24] Parra, F. I. and Ahedo, E., "Fulfillment of the Bohm Condition on the HPHall Fluid-PIC Code," AIAA Paper 2004-3955, July 2004.

[25] Escobar, D., Ahedo, E., and Parra, F. I., "On Conditions at the Sheath Boundaries of a Quasineutral Code for Hall Thrusters," Presented at the 29th International Electric Propulsion Conference, IEPC Paper 2005-041, Princeton, NJ, Oct. 31 - Nov. 4, 2005.

[26] Ahedo, E. and De Pablo, V., "Effects of Electron Secondary Emission and Partial Thermalization on a Hall Thruster Plasma," AIAA Paper 2006-4328, July 2006.

[27] Raitses, Y., Staack, D., Smirnov, A., and Fisch, N. J., "Space Charge Saturated Sheath Regime and Electron Temperature Saturation in Hall Thrusters," Physics of Plasmas **12**, 073507 (2005).

[28] Kaganovich, I. D., Raitses, Y., Sydorenko, D., and Smolyakov, A., "Kinetic Effects in Hall Thruster Discharge," AIAA Paper 2006-4831, July 2006.

[29] Taccogna, F., Longo, S., and Capitelli, M., "Plasma Sheaths in Hall Discharge," Physics of Plasmas **12**, 093506 (2005).

[30] Kim, V., Kozlov, V., Skrylnikov, A., Veselovzorov, A., Hilleret, N. et al., "Investigation of Operation and Characteristics of Small SPT with Discharge Chamber Walls Made of Different Ceramics," AIAA Paper 2003-5002, July 2003.

[31] Bugeat, J. P. and Koppel, C., "Development of a Second Generation of SPT," Presented at the 24th International Electric Propulsion Conference, IEPC Paper 1995-35, Moscow, Russia, Sept. 19-23, 1995.

[32] Dunaevsky, A., Raitses, Y., and Fisch, N. J., "Secondary Electron Emission from Dielectric Materials of a Hall Thruster with Segmented Electrodes," Physics of Plasmas **10**, 6, 2574-2577 (2003).

[33] Ahedo, E., "Presheath/Sheath Model with Secondary Electron Emission from Two Parallel Walls," Physics of Plasmas **9**, 10, 4340-4347 (2002).

[34] Hobbs, G. D. and Wesson, J. A., "Heat Flow through a Langmuir Sheath in the Presence of Electron Emission," Plasma Physics **9**, 85-87 (1967).

[35] Hofer, R. R. and Gallimore, A. D., "High-Specific Impulse Hall Thrusters, Part 1: Influence of Current Density and Magnetic Field," Journal of Propulsion and Power **22**, 4, 721-731 (2006).

[36] Hofer, R. R. and Gallimore, A. D., "High-Specific Impulse Hall Thrusters, Part 2: Efficiency Analysis," Journal of Propulsion and Power **22**, 4, 732-740 (2006).

[37] Haas, J. M., "Low-Perturbation Interrogation of the Internal and near-Field Plasma Structure of a Hall Thruster Using a High-Speed Probe Positioning System," Ph.D. Dissertation, Aerospace Engineering, University of Michigan, 2001.

[38] Linnell, J. A., "An Evaluation of Krypton Propellant in Hall Thrusters," Ph.D. Dissertation, Aerospace Engineering, University of Michigan, 2007.

[39] Meezan, N. B., Hargus, W. A., and Cappelli, M. A., "Anomalous Electron Mobility in a Coaxial Hall Discharge Plasma," Physical Review E **63**, 026410, 1-7 (2001).

[40] Ivanov, A. A., Ivanov, A. A., and Bacal, M., "Effect of Plasma-Wall Recombination on the Conductivity in Hall Thrusters," Plasma Physics and Controlled Fusion **44**, 1463-1470 (2002).

[41] Bishaev, A. M. and Kim, V., "Local Plasma Properties in a Hall-Current Accelerator with an Extended Acceleration Zone," Soviet Physics Technical Physics **23**, 9 (1978).

[42] Hagelaar, G. J. M., Bareilles, J., Garrigues, L., and Boeuf, J. P., "Two-Dimensional Model of a Stationary Plasma Thruster," Journal of Applied Physics **91**, 9 (2002).

[43] Choueiri, E. Y., "Plasma Oscillations in Hall Thrusters," Physics of Plasmas **8**, 4, 1411-1426 (2001).

[44] Janes, G. S. and Lowder, R. S., "Anomalous Electron Diffusion and Ion Acceleration in a Low-Density Plasma," Physics of Fluids **9**, 6 (1966).

[45] Meezan, N. B. and Cappelli, M. A., "Kinetic Study of Wall Collisions in a Coaxial Hall Discharge," Physical Review E **66**, 036401, 1-10 (2002).

[46] Ahedo, E., Gallardo, J. M., and Martinez-Sanchez, M., "Effects of the Radial Plasma-Wall Interaction on the Hall Thruster Discharge," Physics of Plasmas **10**, 8, 3397-3409 (2003).

[47] Hagelaar, G. J. M., Bareilles, J., Garrigues, L., and Bouef, J. P., "Role of Anomalous Electron Transport in a Stationary Plasma Thruster Simulation," Journal of Applied Physics **93**, 1, 67-75 (2003).

[48] Koo, J. W. and Boyd, I. D., "Modeling of Anomalous Electron Mobility in Hall Thrusters," Physics of Plasmas **13**, 033501 (2006).

[49] Boniface, C., Garrigues, L., Hagelaar, G. J. M., Bouef, J. P., Gawron, D. et al., "Anomalous Cross Field Electron Transport in a Hall Effect Thruster," Applied Physics Letters **89**, 161503 (2006).

[50] Garrigues, L., Hagelaar, G. J. M., Boniface, C., and Bouef, J. P., "Anomalous Conductivity and Secondary Electron Emission in Hall Effect Thrusters," Journal of Applied Physics **100**, 123301 (2006).

[51] Kim, V., Grdlichko, D., Kozlov, V., Lazourenko, A., Popov, G. et al., "Local Plasma Parameter Measurements by Nearwall Probes inside the SPT Accelerating Channel under Thruster Operation with Kr," AIAA Paper 2002-4108, July 2002.

[52] Dorval, N., Bonnet, J., Marque, J. P., Rosencher, E., Chable, S. et al., "Determination of the Ionization and Acceleration Zones in a Stationary Plasma Thruster by Optical Spectroscopy Study: Experiments and Model," Journal of Applied Physics **91**, 8, 4811-4817 (2002).

[53] Kim, S. W., "Experimental Investigations of Plasma Parameters and Species-Dependent Ion Energy Distribution in the Plasma Exhaust Plume of a Hall Thruster," Ph.D. dissertation, Aerospace Engineering, University of Michigan, 1999.